Synthesis of Extended Nanoscale Optical Encoders

Charles E. Wickersham,[†] Daniel H. S. Kerr,[†,‡] and Everett A. Lipman*[,†,§]

Department of Physics, University of California, Santa Barbara, California 93106, United States, College of Creative Studies, University of California, Santa Barbara, California 93106, United States, and Biomolecular Science and Engineering Program, University of California, Santa Barbara, California 93106, United States. Received May 2, 2010; Revised Manuscript Received September 22, 2010

An optical encoder is a device that uses an interrupted light source−sensor pair to map linear or rotational motion onto a periodic signal. Simple, inexpensive optical encoders are used for precise positioning in machines such as desktop printers, disk drives, and astronomical telescopes. A strand of DNA labeled with a series of Förster resonance energy transfer acceptor dyes can perform the same function at the nanometer scale, producing a periodic fluorescence signal that encodes the movement of a single donor-labeled molecular motor with high spatial and temporal resolution. Previous measurements of this type have employed encoders limited to five acceptor dyes, and hence five signal periods, restricting the range of motion that could be followed. Here we describe two methods for synthesizing double-stranded DNA containing several to hundreds of regularly spaced dyes on one strand. Distinct functional groups incorporated at the encoder ends enable tethering for single-molecule measurements.

INTRODUCTION

Single-molecule Förster resonance energy transfer (FRET) (*1, 2*) is a powerful technique for measuring nanoscale distances between two fluorophores. Its high sensitivity in the range of approximately 2−10 nanometers is ideal for the study of structural rearrangements in biological macromolecules (*3*−*5*). Until recently, single-molecule FRET measurements of processive motor proteins on DNA (*6*−*9*) have been limited by the presence of only one or a few dye pairs to examination of a restricted range of motion. Furthermore, it remains difficult to obtain accurate distances from measured FRET efficiencies (*10*−*13*).

Precise measurements of macroscopic motion are often made by mapping distance and velocity onto the phase and frequency of a periodic signal. This can be done using an optical encoder, in which a light source and sensor move with respect to a mask containing regularly spaced transparent windows. As the source and sensor move, the window pattern modulates the sensor output, producing the desired signal. We recently implemented a nanoscale encoder (*2, 14*) using FRET between a moving donor fluorophore and a series of acceptors attached to one strand of a DNA molecule at 69 base pair (bp) intervals. As a donor-labeled helicase traveled along the FRET encoder, a periodic acceptor fluorescence signal was observed.

We synthesized the original five-period FRET encoders from 12 unique self-assembling DNA oligonucleotides. While this scheme has the advantage of producing a well-defined product, its cost and complexity both increase with the length of the encoder. To follow translocation over long distances, observe many cycles of the same molecular motor, and collect multiple periods of any signal modulation (*14*), it is desirable to have encoders many times longer than would be practical to synthesize using our original scheme. Here we demonstrate two methods that produce FRET encoders with lengths ranging from several to hundreds of periods.

The first method employs polymerization-driven self-assembly (*15, 16*). We designed two synthetic oligonucleotides that, when annealed, form a double-stranded DNA monomer with two complementary cohesive ends. Upon annealing, the monomers undergo a step polymerization reaction that rapidly produces a wide distribution of encoder lengths.

The second method exploits rolling circle amplification (*17*) (RCA), a process used in the replication of many bacterial plasmids (*18*), in bacterial conjugation (*19*), and by many retroviruses (*20*) and bacteriophages (*21*). In RCA (Figure 4), a suitable polymerase binds to a primed single-stranded circular template. DNA synthesis begins from the 3′ terminus of the primer and proceeds around the circle, generating a linear complement to the circular template. After the polymerase completes one revolution around the template, the newly synthesized strand is removed by a cooperating helicase, or by the polymerase itself, so that the process can continue. Because of its extreme processivity and strand displacement ability, DNA polymerase from the ϕ29 bacteriophage is particularly suitable for RCA (*22*).

RCA has found many uses in nanotechnology (*23*), mutation detection (*24*), and immunoassays (*25*). Recently, two groups (*26, 27*) used RCA to generate periodic double-stranded DNA templates, on which they assembled arrays of gold nanoparticles. We have adapted this technique to synthesize FRET encoders with more than 200 periods, terminated with biotin and digoxigenin groups for site-specific immobilization in single-molecule experiments.

EXPERIMENTAL PROCEDURES

Buffers and Reagents. All solutions were prepared in distilled deionized water (DDI). DNA was stored in 10 mM Tris-HCl (pH 8.0) with 1 mM EDTA (TE buffer). Gels were cast and run in 40 mM Tris-acetate and 1 mM EDTA. Fluorescence measurements were performed in a fluorescence buffer containing 50 mM Tris-HCl (pH 7.9), 1 mM EDTA, 10 mM NaCl, 10 mM $MgCl_2$, 4 mM dithiothreitol, and an enzymatic oxygen-scavenging system consisting of 35 μg/mL

* To whom correspondence should be addressed. E-mail: lipman@physics.ucsb.edu.

[†] Department of Physics, University of California.

[‡] College of Creative Studies, University of California.

[§] Biomolecular Science and Engineering Program, University of California.

10.1021/bc100215j
Published on Web 11/11/2010

Table 1. FRET Encoder Single-Stranded Oligonucleotide Sequences[a]

name	nucleotide sequence (5′ → 3′)
a-b	TTCTTGCACCAGTGTCCTCTCCGCGTCGTCCTACAG TGACTAGTCTGGAACGTATAGTATAAGC
A-B	GACACTGGTGCAAGAAGCTTATACTATACGTTCCA GACTAGTCACTGTAGGACGACGCGGAGAG
a-z-p	TTCTTGCACCAGTGTCCAATATGCAGAACGATCCAA GACGCAATAGCTCC
a-b10	TTCTTGCACCAGTGTCCTCTCCGCGT

[a] The primer−template complex (A-B−a-b10) melts at 74 °C in 100 mM NaCl.

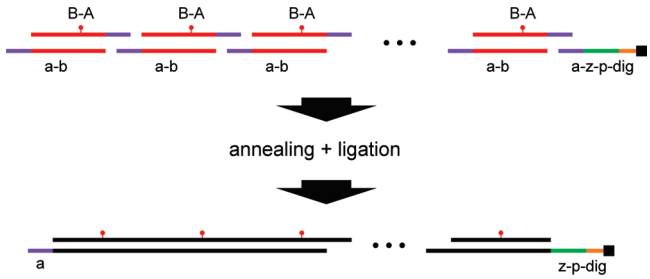

Figure 1. Schematic representation of the polymerizing FRET encoder. The fully assembled encoder consists of a series of regularly spaced FRET acceptor dyes on a double-stranded DNA scaffold. The acceptors are located between bases 32 and 33 of oligo A-B (read 5′ to 3′), and in the final product are spaced by 64 base pairs, approximately four times the Förster radius (R_0) when used with a typical donor dye. An increase in the amount of oligo a-z-p, which binds to unoccupied "A" sites and leaves an unmatched 34-nucleotide cohesive end, will limit the degree of polymerization.

catalase (Sigma-Aldrich C100), 0.2 mg/mL glucose oxidase (Sigma-Aldrich G2133), 0.8% (w/v) D-glucose (Sigma-Aldrich G8270), and 1.2 mM Trolox antioxidant (Sigma-Aldrich 238813) (*28*). Reaction buffers for T4 ligase, ϕ29 polymerase, and terminal transferase were supplied by the manufacturer (New England Biolabs, Ipswich, MA).

DNA Sequences. Sequences for the single-stranded oligonucleotides used in both synthesis schemes are listed in Table 1. All DNA was purchased from Integrated DNA Technologies (Coralville, IA). Oligos A-B and a-b were PAGE purified, and oligo A-B-Cy5, identical to oligo A-B except for a Cy5 fluorophore between bases 32 and 33, was purified by HPLC. All sequences other than a-z-p and a-b10 (the primer for rolling circle amplification reactions) have a 5′ phosphate to enable ligation. To allow for attachment of completed encoders in single-molecule experiments, oligo a-b10 has a 5′ biotin modification, and the terminating oligo a-z-p has a 3′ digoxigenin.

FRET Encoder Synthesis by Polymerization. For polymerization-driven self-assembly, we designed the two partially complementary 64-base oligonucleotides a-b and A-B listed in Table 1. Together they form a 48 bp double-stranded DNA monomer with two 16-base 5′ cohesive ends (Figure 1). The average molecular weight of the product was controlled by the terminator oligonucleotide a-z-p, which anneals at one end of the growing chain, preventing further polymerization from its binding site. The terminating oligo can be designed to incorporate a binding site for a particular motor protein at one end of the encoder, as well as a hapten or biotin for site-specific immobilization.

To synthesize the encoders, we annealed 50 pmol of oligo a-b, 100 pmol of oligo A-B, and a selected ratio of a-z-p to a-b (Figure 2) in a total volume of 8 μL of TE buffer containing

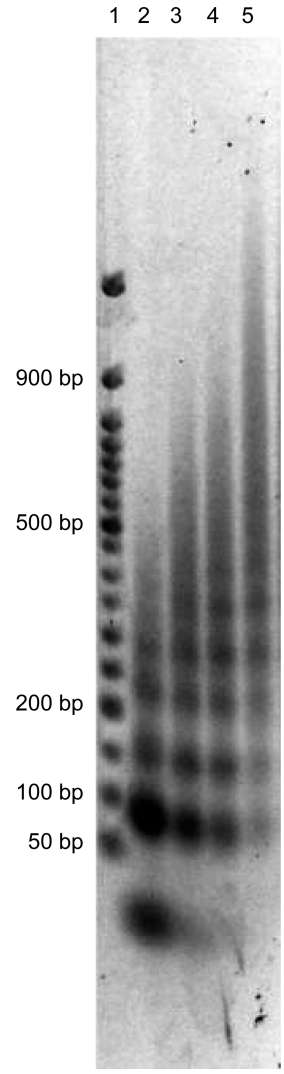

Figure 2. Tuning the molecular weight distribution with a terminator oligonucleotide. The left lane contained a 50 bp DNA marker ladder. The encoders in lanes 2, 3, 4, and 5 were annealed and ligated with 10:1, 2:1, 1:1, and 1:5 molar ratios of oligo a-z-p to monomers, respectively.

100 mM NaCl. When the ratio of a-b to A-B was varied (Figure 3), 50 pmol of a-b was used and the a-z-p terminator was omitted until after the encoders had been separated by size and purified. The mixtures were heated to 65 °C and then cooled to room temperature over the course of approximately 5 min. We connected discontinuous backbone strands in the resulting encoders by adding 1 μL (400 units) of T4 DNA ligase and 1 μL of 10× T4 ligase reaction buffer and incubating overnight at room temperature.

Polymerization results in a broad distribution of FRET encoder lengths. We separated the ligated polymer mixture on a 1.2% (w/v) agarose gel at 160 V for 4.5 h, alongside a 50 bp DNA marker ladder (New England Biolabs). The gel was poststained in a 0.5 μg/mL ethidium bromide solution for 30 min, destained for 30 min in DDI, and visualized using a UV transilluminator. Gel slices were purified using the Wizard Gel Clean-Up kit (Promega, Madison, WI) following the manufacturer's instructions, except that the gel slice was dissolved at room temperature. Heating of the ligated encoders was avoided to prevent melting. Because the DNA sequences are periodic, melting and subsequent reannealing could result in a relative frame shift between the two strands of some integral number of periods.

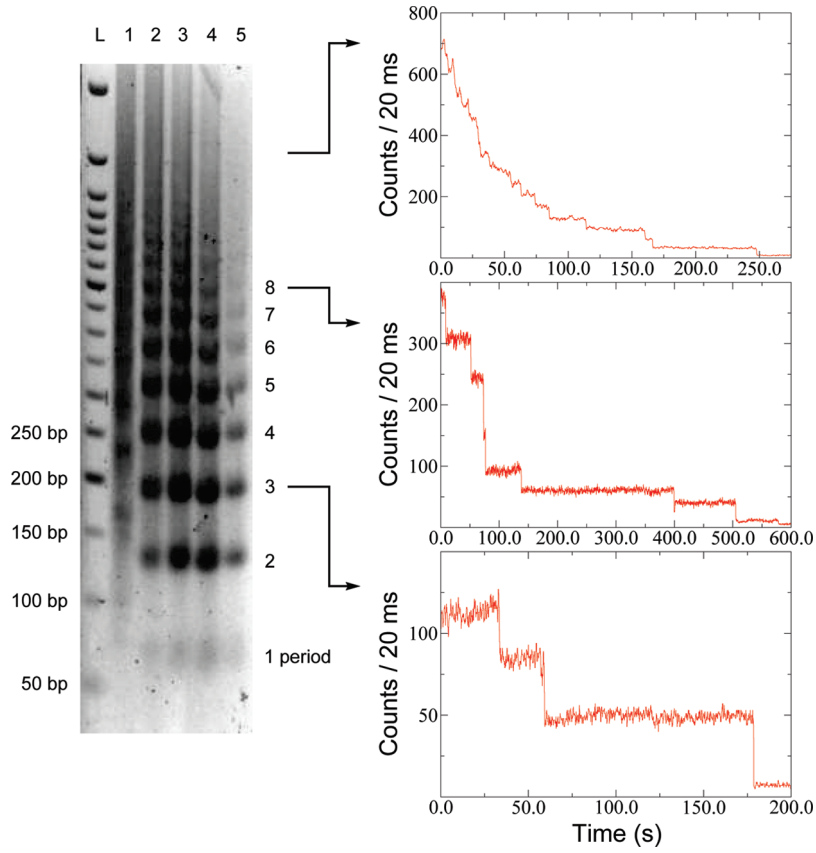

Figure 3. Characterization of polymerized FRET encoders. Agarose gel electrophoresis resolves discrete encoder lengths up to approximately 10 periods. Lane L contained a 50 bp DNA marker ladder. Encoders in lanes 1, 2, 3, 4, and 5 were synthesized with 1:1, 1:2, 1:3, 1:4, and 1:5 ratios of oligo A-B to a-b, respectively. An excess of one monomer oligo over the other improves resolution while preventing the growth of excessively long encoders. Photobleaching traces are shown for FRET encoder DNA extracted from the three- and eight-period bands, and from a position in the gel corresponding to approximately 15 periods. Random temporary drops in the signal are expected from dye blinking (*30*). In the eight-period event, two steps occur near 75 s, while the eighth, smaller step, occurs around 575 s.

FRET Encoder Synthesis by Rolling Circle Amplification. The procedure for RCA patterning is summarized in Figure 4. We formed rolling circle templates by combining 2 μL of 100 μM A-B oligo and 2 μL of 100 μM a-b10 primer in 200 μL of TE buffer containing 100 mM NaCl. We annealed the DNA by heating the solution to 65 °C and then cooling it to room temperature over the course of several hours. This step fully melts undesirable secondary structures in the component oligos, the most stable of which melts at 36.2 °C in 100 mM NaCl. We ligated nicks in the circular templates by adding 1 μL (400 units) of T4 DNA ligase and 21.2 μL of a 10× concentrate of the T4 DNA ligase reaction buffer.

After 3 h of ligation, 30 μL of 10× ϕ29 polymerase reaction buffer, 6 μL of 10 mg/mL bovine serum albumin, 30 μL of 10 mM dNTPs, 30 units of ϕ29 polymerase, and 9 μL of H_2O were added. The reaction mixture was incubated at 31 °C for 3 h, followed by a 10 min 65 °C heat inactivation of the polymerase. The single-stranded RCA product was separated from free nucleotides and the circular templates using a centrifugal filter device (Millipore Ultracel YM-100, 100 kDa NMWL cutoff, Fisher Scientific catalog no. 42412). The 300 μL reaction mixture was diluted to 500 μL with TE buffer and then concentrated to approximately 15 μL. This process was repeated twice more before the DNA was diluted to a final concentration of 75 μL. According to the filter manufacturer's specifications, encoder DNA recovery is expected to be greater than 95%, with more than 99% free nucleotide removal. Preparations for single-molecule measurements select for properly tethered molecules with significant fluorescence. Small residual impurities are either washed out of the flow cell prior to observations or remain undetected.

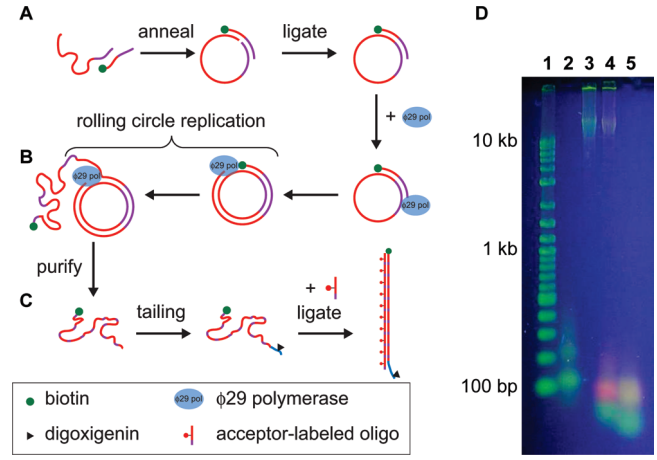

Figure 4. Rolling circle amplification for FRET encoder synthesis. After cyclization of the template by ligation in the presence of a primer (A), an RCA step (B) produces a long concatemer of the complement to the circular template. A tail is appended to the single-stranded product with terminal transferase using dTTP and digoxigenin-labeled dUTP, and subsequent annealing and ligation with the dye-labeled version of the circular template completes a long, bifunctionalized FRET encoder (C). (D) Lane 1 contained a 2 log DNA marker ladder. Lane 2 contained the circular template−primer complex, dimers and trimers of which are also visible. Lane 3 contained the single-stranded RCA product, while lane 4 contained the final annealed and ligated encoder. SpeI, a restriction enzyme that cuts the encoder DNA once per period, was added to the sample from lane 4, which was then run in lane 5. The disappearance of the ≈13 kb double-stranded DNA demonstrates that the encoder is periodic.

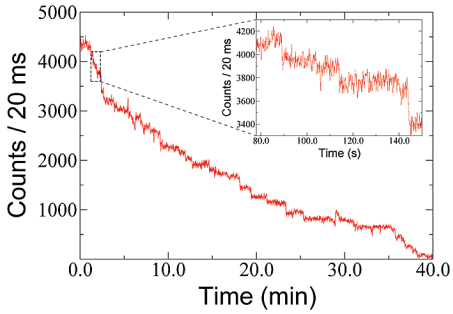

Figure 5. Photobleaching of an immobilized RCA FRET encoder. By eye, we can discern approximately 33 steps. Upward steps, such as those near 29 min and in the inset, are likely caused by the return of a single acceptor (Cy5) from a dark state (*30*). The horizontal position of the focus was adjusted manually in 10 nm increments every few minutes to correct for instrument drift, so that the encoder would remain centered during the 40 min measurement. A 10 nm displacement is only 2.7% of the measured beam waist at the sample plane (data not shown) and could not produce the observed steps.

We appended a digoxigenin-labeled tail to the RCA product by reacting it with terminal transferase in the presence of dTTP and digoxigenin-labeled dUTP. Terminal transferase is a template-independent polymerase that catalyzes the addition of nucleotides to the 3′ end of a strand of DNA. Supplying terminal transferase with a 5−10:1 mixture of dTTP and dig-dUTP produces a tail containing several digoxigenins spaced sufficiently far apart to allow multiple anti-digoxigenins to bind.

For the tailing reaction, 1.7 μg of the purified single-stranded RCA product was combined with 2.5 μL of 10× terminal transferase reaction buffer, 2.5 μL of 2.5 mM $CoCl_2$, 0.25 μL of 100 mM dTTP, 5 μL of 1 mM dig-dUTP, 100 units of terminal transferase (New England Biolabs), and sufficient DDI to yield a total solution volume of 25 μL. The reaction mixture was incubated at 37 °C for 2 h, then heated to 70 °C for a 10 min inactivation.

After the tailing reaction was complete, 12.5 μL of reacted solution was mixed with 10 μL of 100 μM A-B-Cy5 oligo, heated to 65 °C, and then cooled over several hours to room temperature so that dye-labeled oligos would anneal to the long single-stranded template. Once annealed, double-stranded DNA was purified using a PCR spin column (Invitrogen K3100-01) according to the manufacturer's instructions. Finally, nicks in the double-stranded DNA were closed with T4 ligase as described above, and the product was purified again with the same type of spin column.

Fluorescence Measurements. We characterized assembled and purified FRET encoders from both synthesis schemes with a single-molecule photobleaching assay described in detail previously (*14*). We tethered encoders sparsely to the inner surface of a fused-silica flow cell by incubating 50 pM encoder DNA and 1 nM anti-digoxigenin in fluorescence buffer in the cell for 20 min. Excess DNA was then flushed out with fluorescence buffer.

A 633 nm laser, reduced to 1 μW using absorptive neutral density filters, was focused at the fused-silica surface while a piezoelectric stage supporting the cell was scanned in a raster pattern to search for immobilized encoders. When the fluorescence intensity exceeded a designated threshold, indicating the presence of an encoder in the confocal detection volume, the scan was stopped, and the focal position was optimized using an automated centration algorithm (*29*). The encoder was then excited continuously while fluorescence intensity was measured by photon counting and recorded until all dye molecules had been photobleached. Data processed with a 420 ms (21-point) median filter are shown in Figures 3 and 5.

RESULTS AND DISCUSSION

As can be seen in Figure 2, the polymerization scheme produces a distribution of discrete encoder lengths that can be tuned by varying the amount of terminator oligo a-z-p. Figure 3 shows representative photobleaching measurements of polymerized encoders. Sudden, irreversible downward steps in the fluorescence data, each corresponding to the bleaching of a single dye molecule, are clearly evident, and the numbers of dyes counted in this manner correspond to the gel bands from which the encoders were extracted. It is difficult or impossible to identify discrete bands corresponding to lengths beyond 10 periods; however, photobleaching traces for encoders extracted from the high-molecular weight end of the gel indicate that lengths up to at least 15 periods are produced. The typical yield of purified five-period encoder DNA was approximately 1 pmol, making this reaction on the order of 10 times more efficient for this length alone than that described in ref *14*.

Figure 4 shows an agarose gel electrophoresis analysis of the RCA FRET encoders. Lane 2 contained the annealed primer−template complex. Monomeric and multimeric forms, which arise from primer-mediated cross-linking of the template DNA, are visible. The RCA product derived from any of these substrates will contain the same periodic sequence. The gel indicates that the RCA FRET encoders are approximately 13 kb (200 periods) long on average (lanes 3 and 4), and digestion with SpeI, a restriction enzyme that cuts the encoders once per period, demonstrates that they are periodic (lane 5). The red hue of the long DNA in lane 4 arises from annealing with the dye-labeled oligo, the vast excess of which is clearly visible at the bottom of the lane. In lane 5, the 64 bp DNA appears yellow because the stain more efficiently intercalates double-stranded DNA (the mixture of green stain fluorescence and red acceptor fluorescence produces yellow). In lanes 4 and 5, the lower-most band is an unlabeled truncation product left over from the synthesis of the dye-labeled oligo. As it is not fully complementary to oligo a-b, it does not interfere with assembly of the RCA encoder.

Photobleaching data from an RCA encoder are shown in Figure 5. The length of this encoder (approximately 4.4 μm) greatly exceeds the axial extent of the confocal volume. No refocusing was done during the measurement, so the ≈30 observed steps, corresponding to ≈650 nm of encoder contour length, match our expectation for the number of dyes within the region from which fluorescence was collected.

One could envision extending both of the synthesis schemes we have presented to create polymers with much longer repeat lengths. Several synthetic oligonucleotides could be annealed and ligated to form monomers hundreds of base pairs long, and these could be polymerized as described above. Alternatively, an extended substrate for the rolling circle amplification scheme could be fashioned from two or more single-stranded oligos, cyclized by an equal number of primers. Modification of all but one of the primers with 3′ terminal dideoxynucleotides would allow the origin of the RCA reaction to be specified. FRET encoders assembled in this manner could prove useful for measurements taking advantage of multiple acceptors with distinct spectra, or for studying the effects of specific sequences on transcription.

ACKNOWLEDGMENT

We thank Omar Saleh for discussions and advice. This work was supported by the Hellman Family Foundation and the California Nanosystems Institute. E.A.L. is an Alfred P. Sloan research fellow.

LITERATURE CITED

(1) Ha, T., Enderle, T., Ogletree, D. F., Chemla, D. S., Selvin, P. R., and Weiss, S. (1996) Probing the interaction between two single molecules: Fluorescence resonance energy transfer between a single donor and a single acceptor. *Proc. Natl. Acad. Sci. U.S.A. 93*, 6264–6268.

(2) Weiss, S. (1999) Fluorescence spectroscopy of single biomolecules. *Science 283*, 1676–1683.

(3) Deniz, A. A., Laurence, T. A., Dahan, M., Chemla, D. S., Schultz, P. G., and Weiss, S. (2001) Ratiometric single-molecule studies of freely diffusing biomolecules. *Annu. Rev. Phys. Chem. 52*, 233–253.

(4) Zhuang, X. W., and Rief, M. (2003) Single-molecule folding. *Curr. Opin. Struct. Biol. 13*, 88–97.

(5) Schuler, B., and Eaton, W. A. (2008) Protein folding studied by single-molecule FRET. *Curr. Opin. Struct. Biol. 18*, 16–26.

(6) Myong, S., Rasnik, I., Joo, C., Lohman, T. M., and Ha, T. (2005) Repetitive shuttling of a motor protein on DNA. *Nature 437*, 1321–1325.

(7) Myong, S., Bruno, M. M., Pyle, A. M., and Ha, T. (2007) Spring-loaded mechanism of DNA unwinding by hepatitis C virus NS3 helicase. *Science 317*, 513–516.

(8) Verbrugge, S., Lansky, Z., and Peterman, E. J. G. (2009) Kinesin's step dissected with single-motor FRET. *Proc. Natl. Acad. Sci. U.S.A. 106*, 17741–17746.

(9) Christian, T. D., Romano, L. J., and Rueda, D. (2009) Single-molecule measurements of synthesis by DNA polymerase with base-pair resolution. *Proc. Natl. Acad. Sci. U.S.A. 106*, 21109–21114.

(10) Sabanayagam, C. R., Eid, J. S., and Meller, A. (2005) Using fluorescence resonance energy transfer to measure distances along individual DNA molecules: Corrections due to nonideal transfer. *J. Chem. Phys. 122*, 061103.

(11) Braslavsky, S. E., Fron, E., Rodriguez, H. B., Roman, E. S., Scholes, G. D., Schweitzer, G., Valeur, B., and Wirz, J. (2008) Pitfalls and limitations in the practical use of Forster's theory of resonance energy transfer. *Photochem. Photobiol. Sci. 7*, 1444–1448.

(12) Beljonne, D., Curutchet, C., Scholes, G. D., and Silbey, R. J. (2009) Beyond Forster Resonance Energy Transfer in Biological and Nanoscale Systems. *J. Phys. Chem. B 113*, 6583–6599.

(13) Camley, B. A., Brown, F. L. H., and Lipman, E. A. (2009) Förster Transfer Outside the Weak-Excitation Limit. *J. Chem. Phys. 131*, 104509.

(14) Wickersham, C. E., Cash, K. J., Pfeil, S. H., Bruck, I., Kaplan, D. L., Plaxco, K. W., and Lipman, E. A. (2010) Tracking a Molecular Motor with a Nanoscale Optical Encoder. *Nano Lett. 10*, 1022–1027.

(15) Hartley, J. L., and Gregori, T. J. (1981) Cloning multiple copies of a DNA segment. *Gene 13*, 347–353.

(16) Winfree, E., Liu, F. R., Wenzler, L. A., and Seeman, N. C. (1998) Design and self-assembly of two-dimensional DNA crystals. *Nature 394*, 539–544.

(17) Fire, A., and Xu, S. Q. (1995) Rolling replication of short DNA circles. *Proc. Natl. Acad. Sci. U.S.A. 92*, 4641–4645.

(18) Khan, S. A. (1997) Rolling-circle replication of bacterial plasmids. *Microbiol. Mol. Biol. Rev. 61*, 442–455.

(19) Lanka, E., and Wilkins, B. M. (1995) DNA processing reactions in bacterial conjugation. *Annu. Rev. Biochem. 64*, 141–169.

(20) Branch, A. D., and Robertson, H. D. (1984) A replication cycle for viroids and other small infectious RNAs. *Science 223*, 450–455.

(21) Baas, P. D. (1985) DNA replication of single-stranded *Escherichia coli* DNA phages. *Biochim. Biophys. Acta 825*, 111–139.

(22) Blanco, L., Bernad, A., Lazaro, J. M., Martin, G., Garmendia, C., and Salas, M. (1989) Highly efficient DNA-synthesis by the phage ϕ-29 DNA-polymerase: Symmetrical mode of DNA-replication. *J. Biol. Chem. 264*, 8935–8940.

(23) Zhao, W. A., Ali, M. M., Brook, M. A., and Li, Y. F. (2008) Rolling circle amplification: Applications in nanotechnology and biodetection with functional nucleic acids. *Angew. Chem., Int. Ed. 47*, 6330–6337.

(24) Lizardi, P. M., Huang, X. H., Zhu, Z. R., Bray-Ward, P., Thomas, D. C., and Ward, D. C. (1998) Mutation detection and single-molecule counting using isothermal rolling-circle amplification. *Nat. Genet. 19*, 225–232.

(25) Schweitzer, B., Wiltshire, S., Lambert, J., O'Malley, S., Kukanskis, K., Zhu, Z. R., Kingsmore, S. F., Lizardi, P. M., and Ward, D. C. (2000) Immunoassays with rolling circle DNA amplification: A versatile platform for ultrasensitive antigen detection. *Proc. Natl. Acad. Sci. U.S.A. 97*, 10113–10119.

(26) Deng, Z. X., Tian, Y., Lee, S. H., Ribbe, A. E., and Mao, C. D. (2005) DNA-encoded self-assembly of gold nanoparticles into one-dimensional arrays. *Angew. Chem., Int. Ed. 44*, 3582–3585.

(27) Beyer, S., Nickels, P., and Simmel, F. C. (2005) Periodic DNA nanotemplates synthesized by rolling circle amplification. *Nano Lett. 5*, 719–722.

(28) Rasnik, I., McKinney, S. A., and Ha, T. (2006) Nonblinking and long-lasting single-molecule fluorescence imaging. *Nat. Methods 3*, 891–893.

(29) Ha, T., Chemla, D. S., Enderle, T., and Weiss, S. (1997) Single molecule spectroscopy with automated positioning. *Appl. Phys. Lett. 70*, 782–784.

(30) Bates, M., Blosser, T. R., and Zhuang, X. W. (2005) Short-range spectroscopic ruler based on a single-molecule optical switch. *Phys. Rev. Lett. 94*, 108101.

BC100215J